Institute of Physics Publishing Journal of Physics: Conference Series **17** (2005) 154–167
doi:10.1088/1742-6596/17/1/022 Fifth International Conference on Fine Particle Magnetism

Lamellar magnetism: Effects of interface versus exchange interactions of nanoscale exsolutions in the ilmenite-hematite system

S A McEnroe[1], R J Harrison[2], M J Jackson[3], A M Hirt[4], Peter Robinson[1], Falko Langenhorst[5], F Heidelbach[5], Takeshi Kasama[6,7], Andrew Putnis[8], L L Brown[9] and Ute Golla-Schindler[8]

[1]Geological Survey of Norway, Trondheim, Norway, [2]Dept. Earth Sciences, Cambridge University, UK, [3]Institute of Rock Magnetism, University of Minnesota, USA; [4]Institute of Geophysics, ETH, Switzerland, [5]Bayeriches Geoinstitut, Universität Bayreuth, Germany; [6] Frontier Research System, Institute of Physical and Chemical Research, Saitama, Japan; [7]Dept. of Material Science and Metallurgy, University of Cambridge, Cambridge, UK; [8]Institut für Mineralogie, Universität Münster, Münster, Germany; [9]Dept. of Geosciences, University of Massachusetts, Amherst, USA

E-mail:Suzanne.mcenroe@ngu.no

Abstract. We have examined finely exsolved oxides of the hematite-ilmenite solid-solution series found in slowly cooled middle Proterozoic igneous and metamorphic rocks. These oxides impart unusually strong and stable remanent magnetization. Transmission electron microscopy (TEM) analysis shows multiple generations of ilmenite and hematite exsolution lamellae, with lamellar thicknesses ranging from millimeters to 1-2 nanometers. Rock-magnetic experiments suggest that the remanence is thermally locked to the antiferromagnetism of the hematite component of the intergrowths, yet is stronger than expected for a canted antiferromagnetic hematite or coexisting paramagnetic Fe-Ti-ordered **(R** $\bar{3}$**)** ilmenite. In alternating field experiments a stable magnetization is observed in these samples to fields of 100 to 120 mT, indicating that the natural remanent magnetization (NRM) is stable over billions of years. This feature has implications for understanding magnetism of deep rocks on Earth, or on planets like Mars that no longer have a magnetic field. Atomic-scale simulations of an **(R** $\bar{3}$**)** ilmenite lamella in a hematite host, based on empirical cation-cation and spin-spin pair interaction parameters, show that boundary regions of the lamellae are occupied by "contact layers" with a hybrid composition of Fe ions, intermediate between Fe^{2+}-rich layers in ilmenite and Fe^{3+}-rich layers in hematite. In this paper we review current data and explore further the nature of the interface.

1. Introduction

Lamellar magnetism is a recently proposed ferrimagnetic substructure [1,2] suggested to occur at the interfaces between fine precipitates of ilmenite and hematite. Grains of finely exsolved hematite–ilmenite (Fe_2O_3–$FeTiO_3$) have been shown to carry a strong and extremely stable remanent magnetization, suggesting an explanation for some magnetic anomalies in the deep Earth and on planetary bodies that no longer retain a magnetic field [3-6]. Large magnetic anomalies have been mapped by the Mars Global Surveyor in the area above the ancient cratered crust of Mars [7-8]. The

strongest anomalies measured at elevations of 100-200 km have amplitudes up to 1500nT, though the magnetic anomalies observed over the younger Martian terranes are much weaker. The magnetic anomalies, with the lack of a global magnetic field, indicate the magnetization measured is due to memory of an ancient magnetic field i.e., a remanent magnetization. Reasonable models of the large anomalies on Mars require intensely magnetized rocks with average natural remanent magnetization (NRM) of 20 A/m and very large volumes of rock, in 100 km wide and 30 km thick crustal slabs [7-9].

The rocks that produce these anomalies are required to preserve their magnetic properties over billions of years. For that to happen, the magnetic mineral (or minerals) holding the remanent memory need to have a strong temporal stability and high coercivity. It is difficult to use anomalies on Earth as analogs for Mars, because of Earth's strong internal magnetic field, such that many Earth magnetic anomalies have a large component due to the interaction of the magnetic minerals with the inducing field. In rocks with multidomain (MD) magnetite this interaction commonly dominates over the permanent memory of the ancient magnetic field acquired when the metamorphic or igneous rocks cooled through their Néel or Curie temperatures, or grew chemically at lower temperatures.

Diverse rocks with Fe-Ti oxides that have lamellar magnetism have very similar magnetic properties, and the effects are clearly shown in aeromagnetic surveys. In the Proterozoic (~1 billion years) Rogaland area, south Norway, the aeromagnetic signature is dominated by the Bjerkreim-Sokndal layered intrusion (BKS, Figure 1) that covers an area of 250 km^2, and by adjacent hemo-ilmenite bearing anorthosites. Over the BKS intrusion the magnetic anomalies change from magnetic lows (blue) where a remanent vector with negative polarity is dominant; to induced anomalies (red)

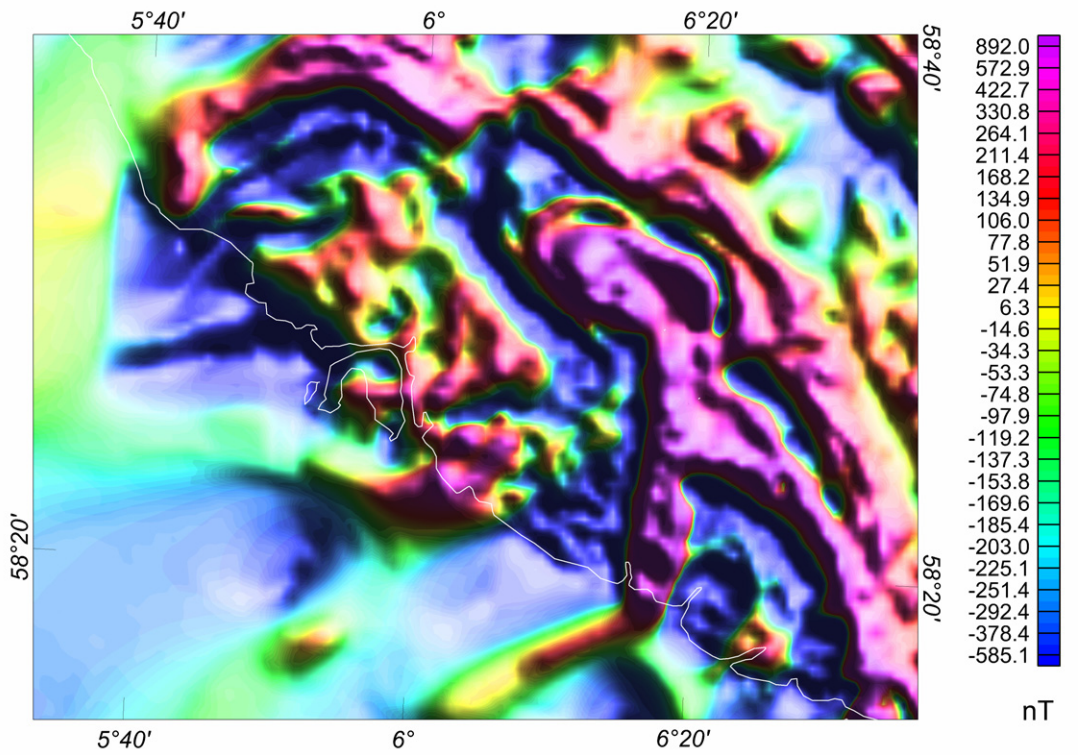

Figure 1. Aeromagnetic map of south Rogaland from a fixed-wing survey. The BKS intrusion forms the large inverted "U" right center. The anomaly values are relative to IGF (1965) reference field. Colour shades: pink = strong positive anomalies; blue = strong negative anomalies; yellow and green = intermediate values. Coastline outlined in white. Scale in nanoteslas, modified from [10]. Image in Figure 2 includes Åna Sira anorthosite (big negative anomaly, lower right) and southeast part of BKS.

with a positive vector dominated by the interaction of the oxide minerals with the present-day magnetic field [10].

The early oxide to crystallize from the magma was ferri-ilmenite that exsolved hematite with cooling. As the magma evolved it became more reduced, leading to crystallization of magnetite, followed by titano-magnetite that exsolved ulvöspinel with cooling. The norite layer in unit IVe in the BKS intrusion contains discrete ilmenite grains with hematite lamellae. Also present are orthopyroxene grains with fine blades of ilmenite with exsolved hematite. Unit IVe forms a very large magnetic anomaly mapped continuously for over 20 km. The most prominent part of the negative anomaly, shown in a high-resolution helicopter survey (Figure 2), with amplitude –13,000 nT and in ground magnetic profiles down to -27,000 nT below background, occurs where cumulate layering is near vertical at the southeast edge of the Bjerkreim Lobe of the intrusion at Heskestad. The shape and magnitude of this anomaly is controlled by the direction of the remanent vector, which is nearly antiparallel to the Earth's present day field [11-12]. Detailed ground-magnetic profiles confirm the near source of the anomaly. Ground-magnetic traverse maps show a low of only 19,000nT in a background of a regional field of 52,000 nT. Samples have natural remanent magnetization intensities of 60 A/m with upward pointing vectors. We successfully model the anomaly using the measured magnetic properties [11].

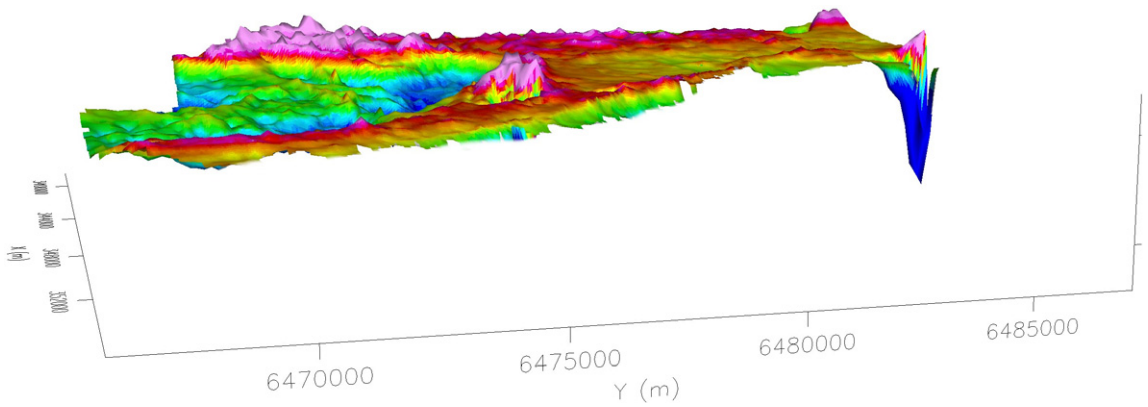

Figure 2. Low angle 3D image with illumination from the east made from the high-resolution helicopter survey data flown over the southern part of the Bjerkreim-Sokndal layered intrusion [modified from 11].

Remanent magnetic anomalies dominate the aeromagnetic surveys over deep-seated Proterozoic rocks of southern Sweden and the Adirondack Mountains, eastern USA [3-6, 13-15], where similar rock properties and exsolution textures have been observed, though in rocks with different oxide bulk compositions and thermal evolution.

Current research is focused the interpretation of aeromagnetic anomalies, on rock-magnetic experiments at all temperatures, observational and analytical transmission electron microscopy (TEM), effects of pressure and compositional variations on the Fe_2O_3–$FeTiO_3$ phase diagram with special emphasis on the magnetic phases, crystal-chemical reconstructions, and additional atomic simulations of lamellar interfaces. Here we review the present data and examine the results of recent experiments aimed at understanding the magnetic properties of fine exsolution lamella and their contact layers.

2. Mineralogy

Common to all the studied areas, where remanent magnetic anomalies dominate the magnetic response of the rocks, are oxide minerals of the hematite-ilmenite (Fe_2O_3-$FeTiO_3$) solid solution series. The relationships between cation ordering, magnetic ordering, and subsolvus exsolution determine the overall magnetic properties in the series [16-18], and of lamellar magnetism in particular.

2.1 Structure and crystal chemistry

Hematite (Fe_2O_3) has the corundum structure (Fig. 3a) with space group $R\bar{3}c$, based on an approximately hexagonal close packed arrangement of oxygen anions, with Fe^{3+} cations occupying 2/3 of the octahedral sites in layers parallel to (001). Ilmenite ($FeTiO_3$) adopts a related structure (space group $R\bar{3}$) (Fig. 3b), with Fe^{2+} and Ti partitioned onto alternating α and β layers. The solid solution contains a mixture of Fe^{2+}, Fe^{3+}, and Ti. Fe^{3+} is distributed equally over the α and β layers at all temperatures and bulk compositions, whereas Fe^{2+} and Ti are partitioned into α and β in ilmenite-rich compositions at low temperatures ($R\bar{3}$) and become randomly distributed over both layers at high temperatures ($R\bar{3}c$).

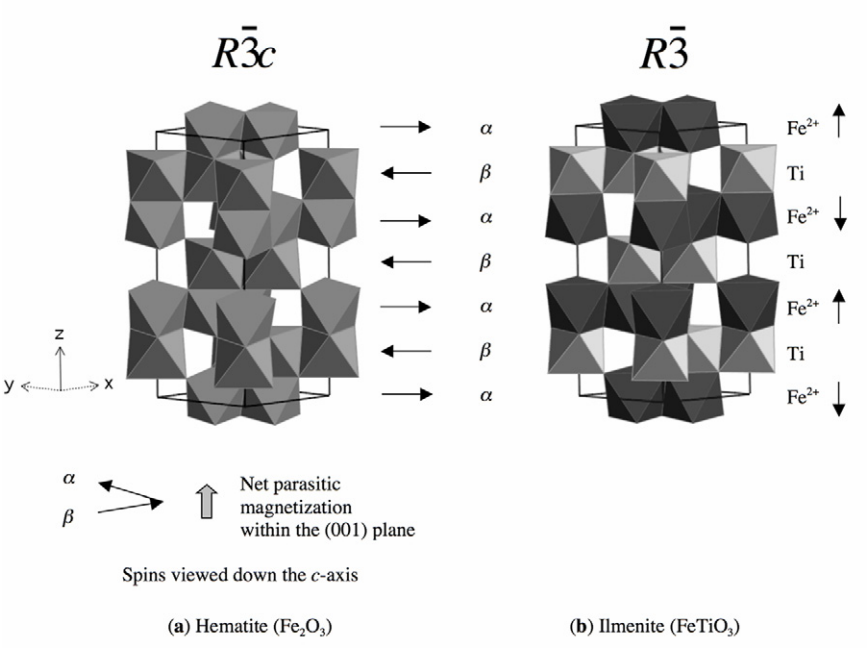

Figure 3. Structure of hematite with alternating layers of Fe^{3+}. Fe is disordered in hematite where it is ordered in ilmenite.

Hematite has a canted antiferromagnetic (CAF) structure with a Néel temperature, T_N = 675 °C. The sublattice spins lie within the basal plane but are rotated by a small angle about [001], producing a weak parasitic magnetic moment perpendicular to the alignment of the spins [19]. End-member ilmenite has an antiferromagnetic structure with spins parallel to [001] and a Néel temperature of ~57 K. Disordered intermediate ilmenites are CAF, with a similar magnetic structure to end-member hematite. Ordered but metastable intermediate ilmenites are ferrimagnetic, because the concentration of Fe on the α and β layers is unequal [16, 20-24].

2.2 Phase diagram

The equilibrium phase diagram at 1 atmosphere (Figure 4) shows the positions of the magnetic- and cation-ordering phase transitions constrained by experimental data [23-26]. The miscibility gap is not well constrained and estimates of its position have been made using different thermodynamic approaches [16-17, 25-30].

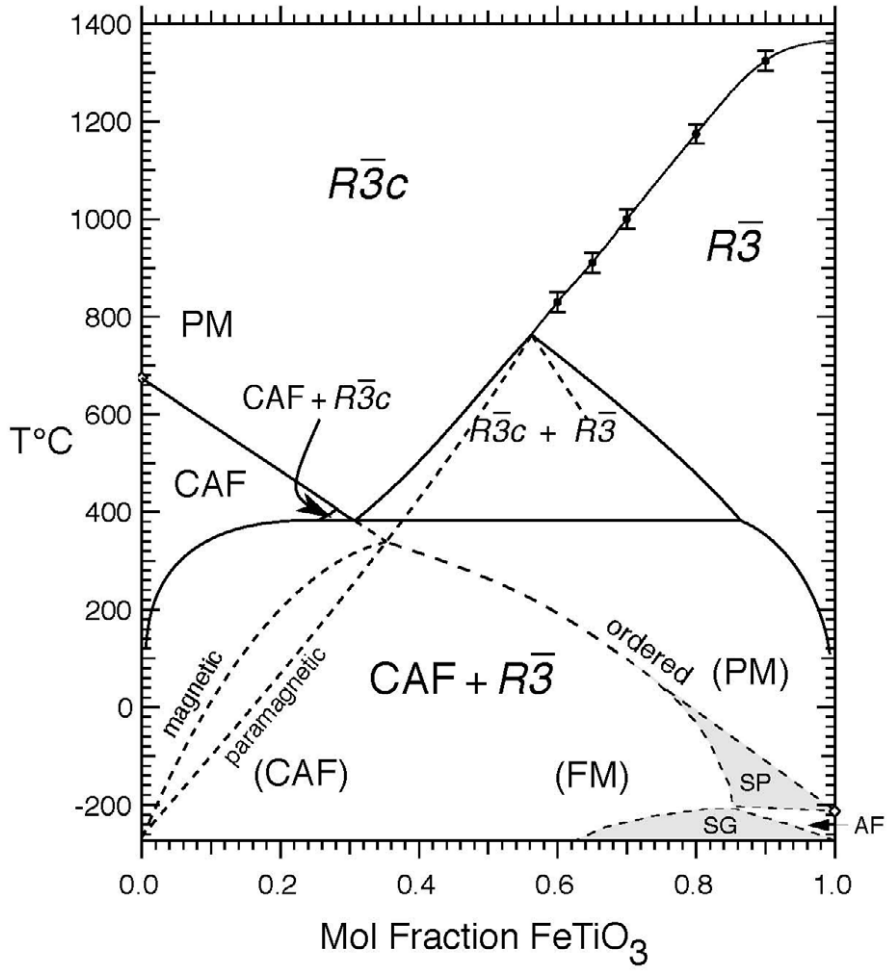

Figure 4. Summary of phase relations in the ilmenite-hematite solid solution at 1 atmosphere: $R\bar{3}c$ = cation disordered; $R\bar{3}$ = cation ordered; P = paramagnetic; CAF = canted antiferromagnetic; FM = ferrimagnetic; AF = antiferromagnetic; SP = superparamagnetic; SG = spin glass. Closed circles are T_{od} for the $R\bar{3}c$ to $R\bar{3}$ phase transition [16, 31]. Endmember T_c's and SP, SG, and AF fields are taken from Ishikawa et al. [23]. The miscibility gap is taken from [30]. Dashed line shows the metastable extension of the magnetic-ordering transition for intermediate compositions quenched from above the miscibility gap. Filled solid areas show regions of superparamagnetic (SP) and spin glass (SG) behavior Modified from Harrison in [5].

Thermodynamic models indicate a miscibility gap below 700-800 °C, separating a paramagnetic hematite-rich phase ($P\ R\bar{3}c$) from a paramagnetic ilmenite-rich phase ($P\ R\bar{3}$). At lower temperatures, the hematite-rich limb of the miscibility gap approaches the magnetic ordering transition, causing the $P\ R\bar{3}c$ phase to become canted AF ($CAF\ R\bar{3}c$). At equilibrium, magnetic ordering in the hematite-rich phase leads to the eutectoid reaction $P\ R\bar{3}c \rightarrow CAF\ R\bar{3}c + P\ R\bar{3}$, and a widening of the gap. The equilibrium state below the eutectoid consists of an intergrowth of $CAF\ R\bar{3}c$ and $P\ R\bar{3}$ phases, with compositions that diverge toward pure hematite and pure ilmenite, so that intermediate- to Ti-rich compositions can be magnetic only below the eutectoid. The size distribution and spatial arrangement

of these phases is a complex function of the cooling history. The natural samples under study crystallized at 5-10 kbar pressure, but pressure effects on phase relations are poorly constrained.

The temperature of the eutectoid reaction has been estimated by several authors using a variety of thermodynamic approaches. Burton [28] used the cluster variation method to determine a value of 525 °C. Ghiorso [30] used a macroscopic thermodynamic model of coupled magnetic and cation ordering to determine a value of 390 °C (this value is used in Figure 4). In the light of new experimental data on the cation ordering phase transition in Ilm60-Ilm100 [16], Harrison and Becker [17] used Monte Carlo simulations to determine a value of 527°C. Further refinements to the model used by Harrison and Becker [17] confirm this value (Harrison, pers. comm.). Given that the approaches used by Burton and Harrison both take proper account of short-range cation and magnetic ordering, our preferred value for the eutectoid temperature is ~ 525 °C.

2.3 Exsolution microstructures

A universal feature of these samples is the abundance of exsolution of ilmenite in hematite hosts, and of hematite in ilmenite hosts [1-6, 14, 32-33]. Optical microscopy and scanning electron microscopy images (Fig. 5) show a range of lamellar thicknesses from several microns down to the limit of these techniques. Observations of exsolution were subsequently made at even higher resolution in transmission electron microscopy (Figures 6, 7), and, using images produced by electron energy loss spectroscopy. The images show that these materials contain abundant lamellar interfaces and that the lamellae continue down to a thickness no more than 1-2 nm, (about one six-layer unit cell of a rhombohedral oxide). Images also show that the interfaces of the finest lamellae are coherent and have considerable lattice strain, a feature that may enhance coercivity and the Curie/Nèel temperature.

Figure 5a. SEM image of Ti-hematite grain with exsolution of ilmenite ($FeTiO_3$) and rutile (TiO_2). Rutile commonly forms as plates or needles and the ilmenite is exsolving on (001) planes of hematite. Scale bar is 2 μm.

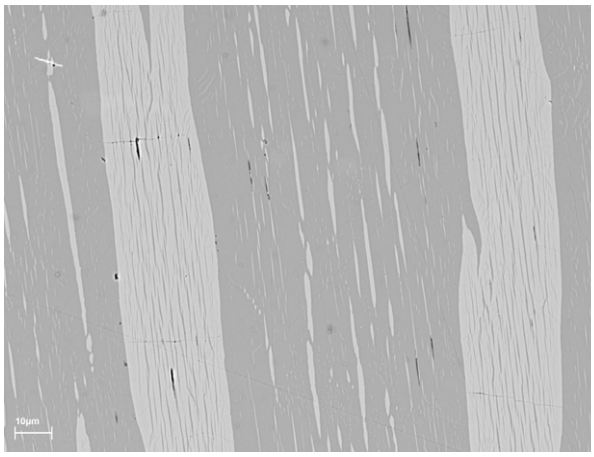

Figure 5b. SEM image of ilmenite ($FeTiO_3$) grain (grey) with exsolution of Ti-hematite (white). First generation hematite lamellae contain abundant later ilmenite lamellae. Scale bar is 10 μm.

The nature, form and distribution of the exsolution lamellae were not known until high-resolution TEM studies were made. Previously our magnetic interpretations of lamella size were based on optical and later SEM images with a resolution of only 100 nm. The nature of fine lamella formation [4-6, 14] left from previous exsolution cycles was a key aspect to the development of the concept of lamellar magnetism. A set of bright field TEM images in Figure 6 shows the development of lamellae in an ilmenite host. Figure 6a shows a coarse early generation hematite lamella most probably originally separated from ilmenite as $R\bar{3}c$ hematite, with subsequent development of fine ilmenite lamellae. Adjacent to the large hematite lamellae in Figure 6a, the ilmenite is homogeneous. With

increasing distance from the hematite lamella, the ilmenite develops a finely mottled texture (Fig. 6b), which in turn develops into discrete fine-scale precipitates of hematite (Fig. 6c) with dark strain shadows in ilmenite near contact interfaces.

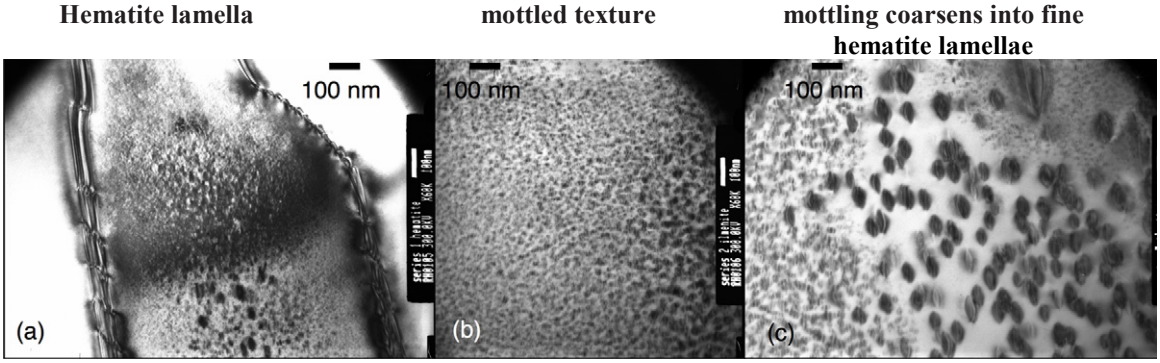

Figure 6. Bright field TEM images of exsolution lamellae in ilmenite host showing relict chemical gradients (from a to c). Scale of exsolution ranges from ~ 1μm to 4nm (modified from [5].

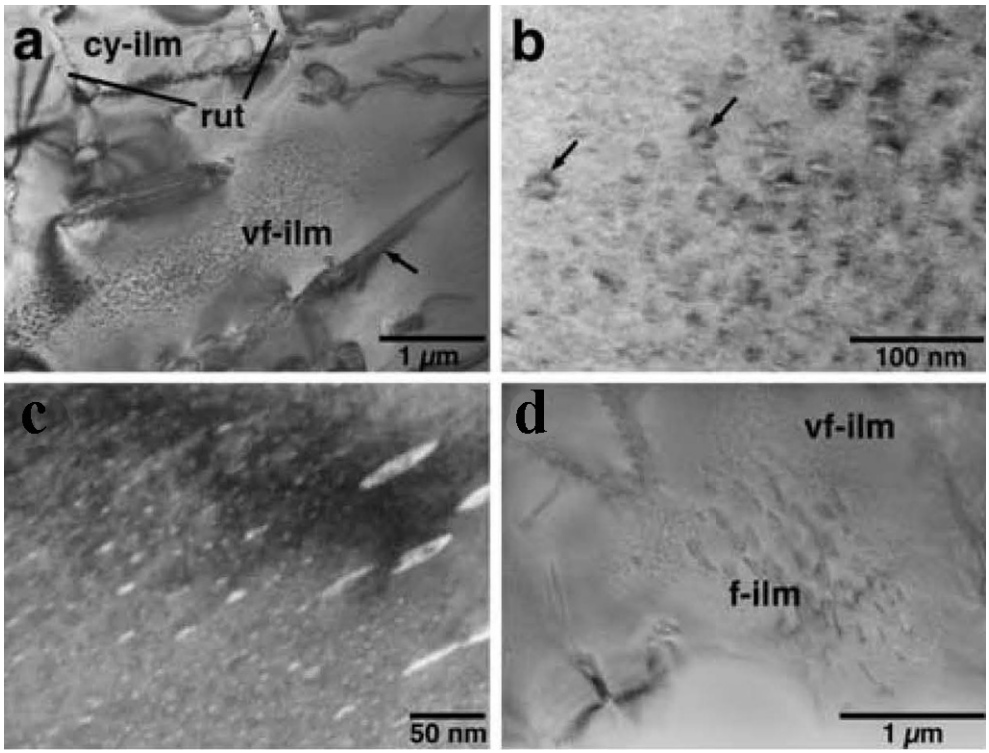

Figure 7. Fine-scale exsolution of ilmenite in hematite host from an Adirondack sample, bright field image for a-c. (a) hematite with large ilmenite lamellae (> 100 nm in width) and abundant very-fine ilmenite lamellae (vf-ilm) and rutile (rut). b) fine and vf- ilmenite lamellae close to end of large ilmenite lamellae. c) hematite with vf- ilmenite lamellae. The arrows indicate a strain contrast between the host and lamellae. d) A dark field image was formed using 003 refection of ilmenite, so that ilmenite appears bright. Figure modified from [6]

The distribution of coarse and fine lamellae, and mottled texture in Figure 6 are interpreted to indicate that there were relict diffusion gradients left from the earlier coarse exsolution process, so that, during later fine exsolution, interior regions reached chemical saturation earliest at highest temperatures whereas exterior regions reached saturation at lowest temperatures, where only mottling occurred. These observations had an important influence in developing models of high lamellar yields, enhancing the possibility for abundant interfaces.

In hematite-rich samples (Figure 5a), there are first-generation ilmenite *PM* $R\bar{3}$ lamellae parallel to (001), and second and subsequent generations of ilmenite *PM* $R\bar{3}$ and hematite lamellae *CAF* $R\bar{3}c$ parallel to (001). In the bright field TEM images of hematite host material (Figure 7) abundant very fine lamellae of ilmenite down to 1-2 nm in thickness are found between the larger 100 nm ilmenite lamellae that were observed on the SEM images. In regions where no discrete larger lamellae are visible, the hematite has developed a very-fine-scale mottling, indicative of chemical heterogeneity on a unit-cell length scale (~1-2 nm). These fine-scale lamellae are always surrounded by strain contrast (arrows in Figure 7b) indicating the interface between the lamellae and host are coherent. The dark-field image shown in figure 7d and electron diffraction patterns revealed that the fine-scale lamellae (smaller than 10 nm in thickness) lie on the (001) planes of the titanium-rich hematite hosts and the interfaces were structurally sharp. The large strain contrast between fine-scale lamellae and the host has been observed in all studies we have made.

Because of the high thermal stability and coercivity of these samples, understanding the nature of the magnetization is also of interest for commercial applications, if the exsolution is reproducible in the laboratory. Common to all samples are grains of ilmenite–hematite with multiple generations of exsolution lamellae, with thicknesses ranging down to unit-cell scale (1–2 nm), about the thickness of one six-layer unit cell of rhombohedral oxide.

3. A new ferrimagnetic substructure

To gain an understanding of how fine-scale exsolution might influence the magnetic properties of these solid solutions, Monte Carlo simulations were made of lamellar interfaces (Fig. 8). Chemical and magnetic interactions of Fe^{2+}, Fe^{3+} and Ti^{4+} ions were studied for nearest- and next-nearest-neighbor locations [1-2, 5-6, 17, 34]. Monte Carlo simulations involved moving individual atoms to new locations, until a picture of individual stable locations formed. Because Ti^{4+} is not paramagnetic, it shields ilmenite Fe^{2+} from magnetic interaction above 57 K. The resultant model has lamellae bounded by "contact layers" parallel to (001). These layers are hybrids of ~half Fe^{2+} ions as in ilmenite and ~half Fe^{3+} as in hematite. Formation of contact layers is proposed to reduce, but not eliminate, electron charge imbalance and lattice strain along interfaces. Figure 8 shows a PM ilmenite lamella within a 24-layer antiferromagnetic hematite. The two contact layers on top and bottom of the lamella have parallel magnetic moments to the left, weaker than hematite Fe^{3+} layer moments, but coupled with them antiferromagnetically. The two contact-layer moments are balanced against one odd hematite layer moment to the right to produce a net magnetic moment per lamella ~4μB to the left. Intensity of lamellar magnetism depends on the proportion of lamellae with parallel magnetic moments (magnetically in phase) and the abundance of exsolution. The proportions of magnetically in-phase lamellae may be enhanced when (001) planes are oriented parallel to the magnetizing field during phase separation. Under perfect in phase-conditions, a lamellar magnetic material could have a saturation magnetization up to 150 kA/m, 70 times stronger than pure hematite, while retaining the high coercivity and thermal properties of single-domain hematite.

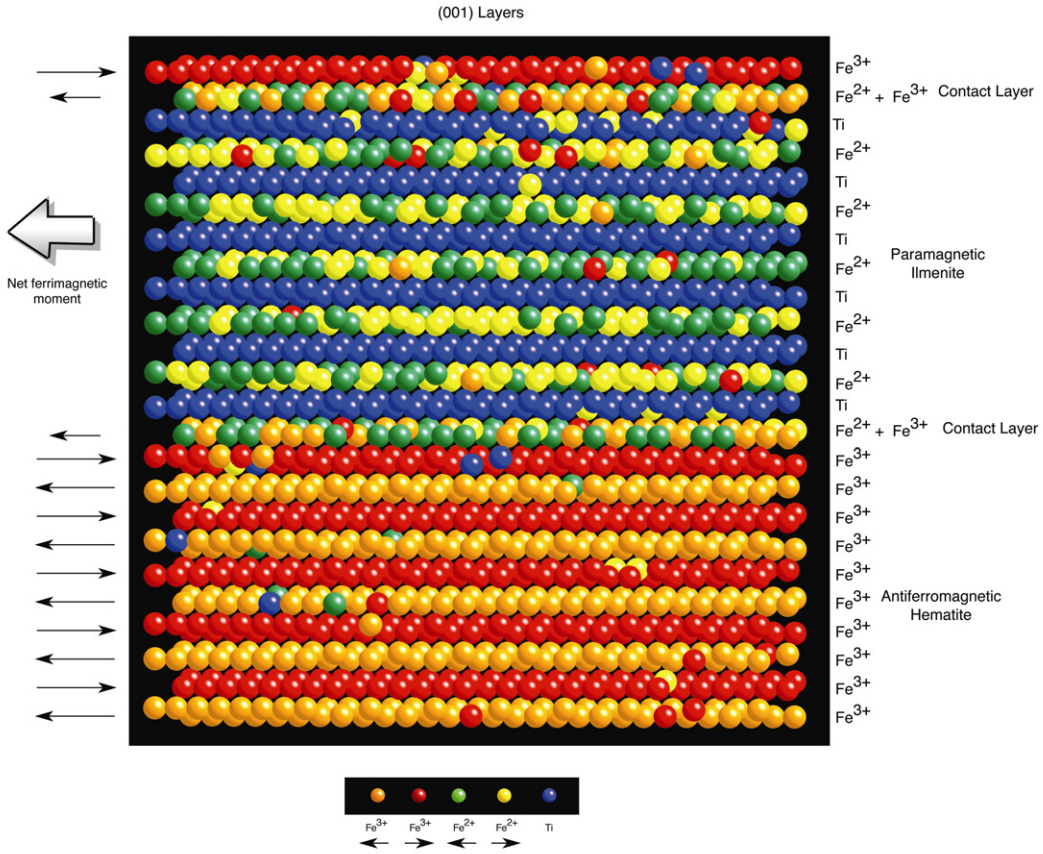

Figure 8. A snapshot of the equilibrium configuration of cations and spins generated below the eutectoid temperature. The lower half of the figure corresponds to cation disordered antiferromagnetic hematite, the upper half to cation ordered paramagnetic ilmenite. The ilmenite lamella is terminated on both sides by a layer Ti, followed by a mixed Fe^{2+}/Fe^{3+} 'contact layer', and finally a layer of Fe^{3+}. This symmetrical termination naturally creates an imbalance between the number of left and right spins, and hence a stable net magnetic moment.

4. Magnetic properties

Samples with exsolution microstructures have magnetic properties that are significantly different from samples that have the same chemical compositions, but do not have exsolution lamellae. All exsolved samples measured, whether the host is ilmenite, or hematite, have high natural remanent magnetizations (NRM). Exsolved samples also show significantly higher medium destructive fields (MDFs) and coercivities than samples that contain only unexsolved oxides. MDFs for samples that contain ilmenite with hematite exsolution are ~70 mT. When hematite is the host grain with ilmenite exsolution MDFs are greater than 100 mT.

In thermal demagnetization experiments, samples all show a high thermal stability (Figure 9). Ilmenite host samples have lower unblocking temperatures than hematite host samples, however all have higher unblocking temperatures than inferred from their hematite compositions measured by TEM.

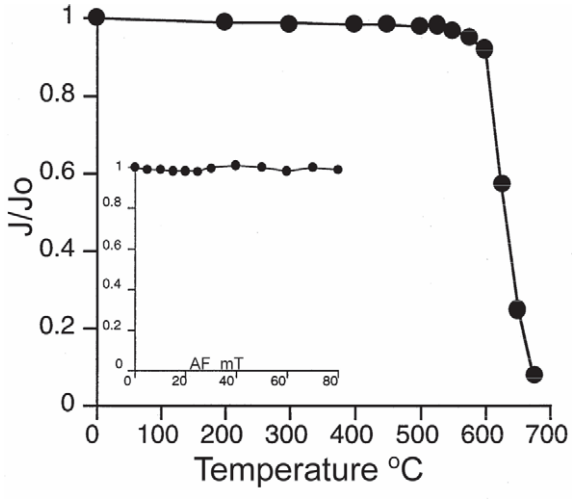

Figure 9. Thermal demagnetization curve of a titanium-rich hematite with exsolution of ilmenite and rutile (see image in figure 5a). J/Jo is the magnetization at each step; either heating up to 670°C, or in an alternating field in 10 mT steps up to 80 mT, normalized to the initial untreated value. All samples show high thermal stability with little loss in magnetization until 600-610°C. Inset shows alternating field demagnetization to 80 mT. Samples are very stable and show no loss in magnetization up to peak field.

Room temperature magnetic hysteresis measurements of ilmenite host samples (Figure 10), with hematite lamellae, that range from a few microns to 1-2 nm, typically have saturation remanence to saturation magnetizations ratios (Mrs/Mr) of ~ 0.2 [35]. These ratios are lower than samples of host hematite with ilmenite lamellae with ratios ~ 0.6 to 0.7 [3 and 6]. Ilmenite host samples with large first generation hematite exsolution, 10µm or greater (figure 5b), have a harder coercivity (Figure 11) than the ilmenite samples with hematite exsolution of only a few µm. In both cases the larger lamellae, from > 10µm to at least as small as 20 nm in thickness are shown to be exsolved.

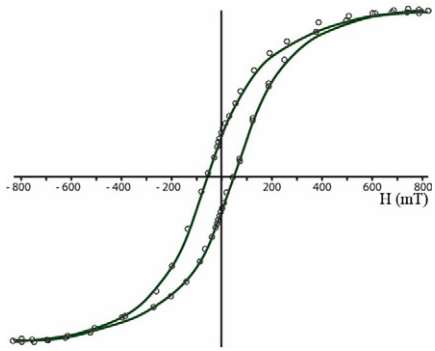

Figure 10. Room temperature hysteresis loops of a paramagnetic ilmenite with hematite lamellae ranging in sizes from ~ 3µm to 1-2 nm in thickness.

Coercivity of saturation (Hc) values for ilmenite host samples are typically between 40 and 70 mT. Hematite host samples have significantly larger Hc values, usually between 150 and 330 mT. Ratios of coercivity of remanence (Hcr) to coercivity of saturation (Hc) in samples of ilmenite host with hematite lamellae are between 2 and 3, whereas hematite hosts with ilmenite lamellae are near 1. These differences are due to the nature of the host, a paramagnetic ilmenite, or an antiferromagnetic hematite. Though there are differences in magnetic properties across the solid solution series, all the exsolved samples studied from this solid solution have relatively high coercivity and NRMs. These properties contrast sharply with those from multidomain hematite samples that have little or no exsolution, where Hc values are much lower, in the range of 3-10 mT [36].

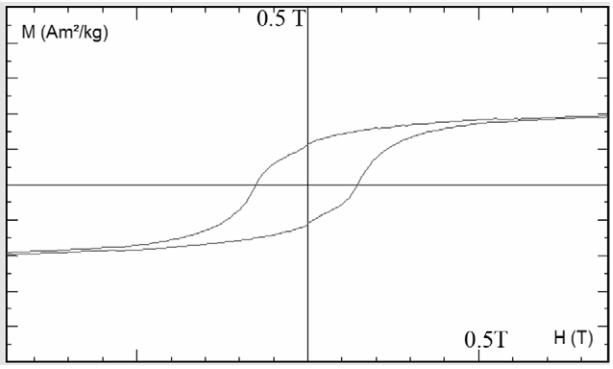

Figure 11. Room temperature hysteresis loop of ilmenite with coarse hematite lamellae (> 10 μm). All hematite lamellae contain abundant nm ilmenite lamellae. Ilmenite host material also contains abundant hematite lamellae, down to a few nm in size. Ms = 100 mA/m; Mr/Ms is 0.61 and Hcr/Hc is 1.1.

Generally magnetic properties of fine particles have strong size dependence. Grains of magnetite and hematite smaller than 30 nm are usually superparamagnetic. In the hematite host samples AC susceptibility measured in multiple frequencies with decreasing temperature indicate that the smallest lamellae are magnetically stable, even though the scale of exsolution, ~1-2 nm, is down to the unit cell size of the material. Mössbauer measurements on ilmenite with micron and nanoscale hematite lamellae shows only magnetically ordered phases [35].

5. Nature of the interface between ilmenite and hematite exsolution

The nature of the interface between the lamellae and the host material has not yet been fully determined. We sought evidence for exchange coupling between lamellae and host phases and designed magnetic experiments to explore this.

Rotational hysteresis (W_R) was determined with a high-field torque magnetometer [37] to investigate whether there is exchange coupling between the antiferromagnetic hematite and the ferrimagnetic contact substructure. The torque of the sample was measured by rotating the sample in progressively higher fields, first by 360° in one direction, and then in the reverse direction. W_R was calculated from the area between the two torque curves. The torque curves are dominated by an asymmetric 2θ-signal, which is characteristic for hematite [38-39]. W_R increases as a function of applied field until reaching a peak between 1200 and 1500 mT and decreasing at higher fields. Vanishing W_R is typical for an anisotropic (anti)ferromagnetic phase that has not reached its saturation field. Above the saturation field W_R will disappear. Samples that undergo exchange interaction show non-vanishing W_R with progressively higher fields.

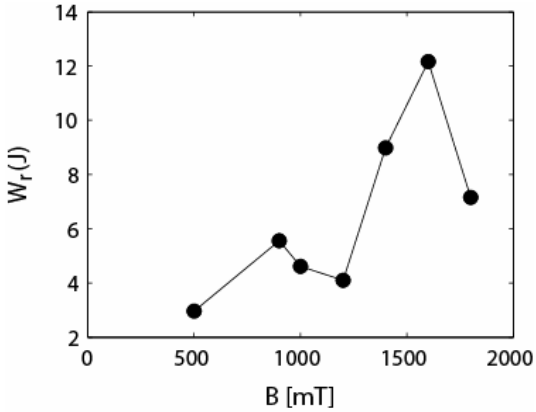

Figure12. Within plane rotational hysteresis

In addition to rotational hysteresis measurements, zero field-cooled and field-cooled hysteresis measurements were made at low temperature to test for the possibility of exchange coupling between

the oxide phases. There was no shift observed between the zero field-cooled and field-cooled hysteresis loops, and the shape of the hysteresis loop is similar to the room temperature hysteresis loop. If exchange coupling were present in these samples then a shift in the hysteresis loop would be expected when the sample is field cooled [40-41].

Because there is a vanishing W_R, and no observed shift in the hysteresis loops, there is at present no evidence for exchange interaction between the hematite, the ilmenite or the ferrimagnetic substructure though all samples contain abundant exsolution lamellae from the micron size down to 1-2 nm. These negative results of tests for exchange coupling in these samples agree with our concept of lamellar magnetism as a single ferrimagnetic substructure related to coherent contacts between hematite and ilmenite regardless of which is the host.

Acknowledgments
SAM is grateful to National Research Council of Norway for funding this work under the Nanomat Program (grant 163556/S10), to the Institute for Rock Magnetism, University of Minnesota for a visiting fellowship and to EU 'IHP-Access to research Infrastructures Program (Contract No. HPRI-1999-CT-00004 to D.C. Rubie).

4. References

[1] Robinson P, Harrison R J, McEnroe S A and Hargraves R 2002 Lamellar magnetism in the hematite-ilmenite series as an explanation for strong remanent magnetization, *Nature* **418** 517-520.

[2] Robinson P, Harrison R J, McEnroe S A and Hargraves R 2004 Nature and origin of lamellar magnetism in the hematite-ilmenite series *American Mineralogist* **89** 725-747.

[3] McEnroe S A and Brown L L 2000 A closer look at remanence-dominated anomalies: Rock-magnetic properties and magnetic mineralogy of the Russell Belt microcline-sillmanite gneisses, Northwest Adirondacks Mountains, New York J. *Geophysical Res.* **105** 16437-16456.

[4] McEnroe S A, Harrison R J, Robinson P, Golla U and Jercinovic M J 2001 The effect of fine-scale microstructures in titanohematite on the acquisition and stability of NRM in granulite facies metamorphic rocks from southwest Sweden: Implications for crustal magnetism *J. Geophysical Res.* **106** 30523-30546.

[5] McEnroe S A, Harrison R J, Robinson Peter and Langenhorst F 2002 Nanoscale haematite-ilmenite lamellae in massive ilmenite rock: an example of lamellar magnetism' with implications for planetary magnetic anomalies *Geophys. J. Int.* **151** 890-912.

[6] Kasama T, McEnroe S A, Ozaki N, Kogure T, and Putnis A 2004 Effects of nanoscale exsolution in hematite-ilmenite on the acquisition of stable natural remanent magnetization. *Earth and Planetary Science Letters* **224** 461-475.

[7] Acuna M H, Connerney J E P, Ness N F, Lin R P, Mitchell D L, Mitchell C W, Carlson J, McFadden J, Anderson K A, Reme H, Mazelle C, Vignes D and Wasilewski P J 1999 Global distribution of crustal magnetization discovered by the Mars Global Surveyor MAG/ER experiment, Science 284 790-793.

[8] Acuna M. H. 2001 The magnetic field of Mars: Summary of results from the aerobraking and mapping orbits. *J. Geophys. Res.* 106 23,403-23,417.

[9] Sprenke K F and L L Baker 2000 Magnetization, paleomagnetic poles and polar wander on Mars. Icarus **14** 26-34.

[10] McEnroe S A, Robinson P and Panish P 2001 Aeromagnetic anomalies, magnetic petrology and rock magnetism of hemo-ilmenite- and magnetite-rich cumulates from the Sokndal Region, South Rogaland, Norway, *American Mineralogist* 86 1447-1468.

[11] McEnroe S A, Skilbrei J R, Robinson P, Heidelbach F, Langenhorst F and Brown L L 2004 Magnetic anomalies, layered intrusions and Mars, *Geophysical Research Letters* **31** *L19601, doi:10.1029/2004GL020640.*

[12] McEnroe S A, Brown L L and Robinson P 2004 Earth analog for Martian magnetic anomalies:

remanence properties of hemo-ilmenite norites in the Bjerkreim-Sokndal intrusion, Rogaland, Norway, *J. Appl. Geophy.* **56** 195– 212.
[13] Balsley J R and A F Buddington 1957 Remanent magnetism of the Russell Belt of gneisses, northwest Adirondack Mountains, New York, *Adv. in Phys.* 6 317- 322.
[14] McEnroe S A, Langenhorst F, Robinson P, Bromiley G and Shaw C 2004 What's magnetic in the lower Crust? *Earth and Planetary Science Letters* 226 175-192.
[15] Balsley J R and A F Buddington 1958 Iron titanium oxide minerals, rocks, and aeromagnetic anomalies of the Adirondack area, New York, *Econ. Geol.* **53** 777-805.
[16] Harrison R J 2000 Magnetic transition in minerals, *Reviews in Mineralogy* **39** 175-202.
[17] Harrison R J and Becker U 2001 Magnetic ordering in solid solutions, *European Mineralogical Union Notes in Mineralogy* **3** *349-383.*
[18] Ishikawa Y and Akimoto S 1957 Magnetic properties of $FeTiO_3$-Fe_2O_3 solid solution series, *J. Phys. Soc. Jpn.* **12** 1083-1098.
[19] Dzialoshinskii I 1958 A thermodynamic theory of "weak" ferromagnetism of antiferromagnetics. *J. Physics and Chemistry of Solids* **4** 241.
[20] Ishikawa Y and Akimoto S 1958 Magnetic property and crystal chemistry of ilmenite ($MeTiO_3$) and hematite (αFe_2O_3) system, I, Crystal chemistry *J. Phys. Soc. Jpn.* **13** 1110-1118.
[21] Ishikawa Y and Akimoto S 1958 Magnetic property and crystal chemistry of ilmenite ($MeTiO_3$) and hematite ($\alpha Fe_2 O_3$) system II. Magnetic property, *J. Phys. Soc. Jpn.* **13** 1298-1310.
[22] Ishikawa Y and Syono Y 1963 Order-disorder transformation and reverse thermo-remanent magnetism in the $FeTiO_3$-Fe_2O_3 system, *J. Phys. Chem. Solids* **24** 517-528.
[23] Ishikawa Y, Saito N, Arai M, Watanabe Y and Takei H 1985 A new oxide spin glass system of (1-x) $FeTiO_3$ - x Fe_2O_3. I. Magnetic Properties, *Journal of the Physical Society of Japan* **54** 312-325.
[24] Harrison R J and Redfern SAT 2001 Short- and long-range ordering in the ilmenite-hematite solid solution, *Phys. Chem. Miner* **28** 399-412.
[25] Harrison R J, Becker U and Redfern SAT 2000. Thermodynamics of the R-3 to R-3c phase transition in the ilmenite-hematite solid solution, *Am. Mineral.* **85** 1694-1705.
[26] Harrison R J, Redfern, SAT, and Smith R I 2000. In-situ study of the R3 to R3c phase transition in the ilmenite-hematite solid solution using time-of-flight neutron powder diffraction. *Am. Mineral.* **85** 194-205.
[27] Burton B P 1984, Thermodynamic analysis of the system Fe_2O_3- $FeTiO_3$, *Phys. Chem. Miner* **11** 132-139.
[28] Burton B P 1985 Theoretical analysis of chemical and magnetic ordering in the system Fe_2O_3-$FeTiO_3$, *Am. Mineral.* **70** 1027-1035.
[29] Burton B P 1991 Interplay of chemical and magnetic ordering, *Reviews in Mineralogy* **25** 303-321.
[30] Ghiorso M S 1997 Thermodynamic analysis of the effect of magnetic ordering on miscibility gaps in the FeTi cubic and rhombohedral oxide minerals and the FeTi oxide geothermometer, *Phys. Chem. Miner.* **25** 28-38.
[31] Harrison R J, Redfern, SAT, and Smith R I 2000. In-situ study of the R3 to R3c phase transition in the ilmenite-hematite solid solution using time-of-flight neutron powder diffraction. *Am. Mineral.* **85** 194-205.
[32] Kasama T, Golla-Schindler U and Putnis A 2003 High-resolution energy-filtered TEM of the interface between hematite ilmenite exsolution lamellae: relevance to the origin of lamellar magnetism, *Am. Mineral.* **88** 1190–1196.
[33] Golla U and Putnis A 2001 Valence state mapping and quantitative electron spectroscopic imaging of exsolution in titanohematite by energy filleted TEM, Phys Chem Miner **28** 119-129.
[34] Burton, BP, Chaka A and Singh D H, 2005 Chemical, magnetic and charge ordering in the system

hematite-ilmenite, $Fe_2O_3 - FeTiO_3$ Phase Transitions **78** 239-249.
[35] Dyar D M, McEnroe S A, Murad E, Brown L L and Schiellerup H 2004 The relationship between exsolution and magnetic properties in hemo-ilmenite: Insights from Mössbauer spectroscopy, *Geophysical Res. Letters* **31** 4 L04608. *doi:10.1029/2003GL019076.*
[36] Halgedahl S L 1998 Barkhausen jumps in large versus small platelets of natural hematite, J. Geophys. Res. **103** 30,575-30,589.
[37] Bergmüller F, Bärlocher C, Geyer B, Grieder, F, Heller F and Zweifel P 1994 A torque magnetometer for measurements of the high-field anisotropy of rocks and crystals, *Meas. Sci. Technol.* **5** 1466-1470.
[38] Porath H and Chamalaun F H 1966 The magnetic anisotropy of hematite bearing rocks, *Pure Appl. Geophys.* **64** 81-88.
[39] Martín-Hernández F and Hirt A M 2004 A method for the separation of paramagnetic, ferrimagnetic and haematite magnetic subfabrics using high-field torque magnetometry, *Geophys. J. Int.* **157** 117-127.
[40] Meiklejohn W H 1962 Exchange Anisotropy, A Review, J. Appl. Phys. **33** 1328-1335.
[41] Nogués J and I K Schuller 1999 Exchange bias, J Magnetism and magnetic Materials **192** 203-232.